BF_3 Adsorption on Stoichiometric and Oxygen-Deficient $SnO_2(110)$ Surfaces

Mark W. Abee and David F. Cox*

Department of Chemical Engineering, Virginia Polytechnic Institute & State University, Blacksburg, Virginia 24061

Received: July 31, 2002; In Final Form: November 25, 2002

BF_3 has been used as a probe of the basicity of surface oxygen anions on $SnO_2(110)$ surfaces. BF_3 interacts directly with surface lattice oxygen "base" sites on $SnO_2(110)$ and acts as a reasonable molecular chemisorption probe for the basicity of thermally stable three-coordinate O^{2-} anions by forming a Lewis acid/base adduct with these particular surface oxygen anions. However, BF_3 reacts irreversibly with the more labile two-coordinate bridging oxygen on the stoichiometric surface, and no distinctive BF_3 desorption feature is observed in thermal desorption that can be used to provide a measure of the basicity of bridging oxygen anions. These results are indicative of an inherent limitation in the application of BF_3 thermal desorption measurements as a simple probe for the basicity of surface oxygen species of limited thermal stability. The presence of bridging oxygen on the stoichiometric surface does gives rise to gas-phase reaction products (HF and F_2) in thermal desorption that are not seen on the more oxygen-deficient surfaces. For all surfaces, some BF_3 dissociation is observed, which results in the slow build up of surface boron and fluoride during consecutive thermal desorption runs.

I. Introduction

The nature of acidic and basic sites on oxide surfaces can be described in both Lewis and Brønsted terms. For clean metal oxide surfaces (no surface protons), the properties are principally described in terms of Lewis acidity and basicity. On metal oxides, coordinately unsaturated metal cations are generally thought of as Lewis acid sites, whereas the oxygen anions are thought of as Lewis base sites.[1,2] The electron-deficient metal cations exhibit acidic, electron-acceptor character, whereas the electron-rich oxygen anions exhibit basic, electron-donor character.[1,2]

Carbon dioxide is commonly used as an acidic probe molecule for characterizing the basicity of oxide surfaces.[3−9] The interaction of carbon dioxide with an oxide surface can be viewed simplistically as an acid/base reaction between a basic oxide ion and acidic CO_2 to form a surface carbonate: $CO_2 + O^{2-} \rightarrow CO_3^{2-}$. This simplistic view tends to ignore the detail that variations in the coordination of CO_2 with an oxide surface make it a nonspecific probe. For example, the formation of a bidentate carbonate surface species likely requires the interaction of CO_2 with neighboring cations and oxide anions (i.e., a site pair[9]), whereas the formation of a monodentate carbonate may require only a direct interaction with a surface oxide anion.[9] In addition, other conformations of adsorbed CO_2 are possible, such as bent $CO_2^{\delta-}$ anions at metal centers and linear unperturbed physisorbates.[10−12] Given the variety of possible coordination geometries for adsorbed CO_2, it is clear that heats of adsorption or activation energies for desorption that characterize the strength of the adsorbate/surface interaction do not, in general, provide a simple measure of a single unique surface property that is readily attributable to surface basicity.

The atomic viewpoint of cations and anions as Lewis acid and base sites suggests that a method for probing the properties of these individual atomic sites would be useful. Given the variety of different coordination environments of oxide anions that may be encountered on different metal oxide materials or different surface orientations of the same material, a probe molecule capable of providing a measure of the basicity (i.e., electronic properties) of individual atomic anion sites on oxide surfaces could prove useful. We have recently used BF_3, a strong Lewis acid, as a probe for the Lewis basicity of surface oxide anions on $Cr_2O_3(10\bar{1}2)$.[13] Thermal desorption experiments indicate that terminal chromyl oxide ions on the oxygen-terminated surface (formed by the dissociative adsorption of O_2) are stronger Lewis base sites than three-coordinate oxide ions on the stoichiometric surface.[13] CO_2 thermal desorption experiments suggest the opposite trend, but coordination differences associated with the bidentate and monodentate adsorbates formed on the stoichiometric and oxygen-terminated surfaces, respectively, make the interpretation of the results in simple acid/base terms for CO_2 difficult.

In the previous study of BF_3 adsorption on $Cr_2O_3(10\bar{1}2)$,[13] the Lewis basicity of three-coordinate and single-coordinate (terminal) oxide species was characterized. In the case of Cr_2O_3, both of these surface oxide species are thermally stable in ultrahigh vacuum to over 1200 K in vacuum.[9] In the present study with $SnO_2(110)$, the surface can be prepared to expose three-coordinate (in-plane) and two-coordinate (bridging) oxide surface species in a controlled fashion. Of these two types of surface oxide anions, the two-coordinate bridging oxygens are labile and can be removed by heating to temperatures of 650 K or less. This investigation will allow a first look at the interaction of BF_3 with two-coordinate bridging oxygen as well as the interaction of BF_3 with oxide anions of dissimilar thermal stability.

II. $SnO_2(110)$ Surfaces Studied

Characterizations of the $SnO_2(110)$ surface have been reported in detail elsewhere.[14−23] Combinations of ion bombardment and oxidation/reduction treatments can be used to prepare surfaces

* Corresponding author. E-mail: dfcox@vt.edu. Fax: (540) 231-5022.

10.1021/jp021771n CCC: $25.00
Published on Web 02/01/2003

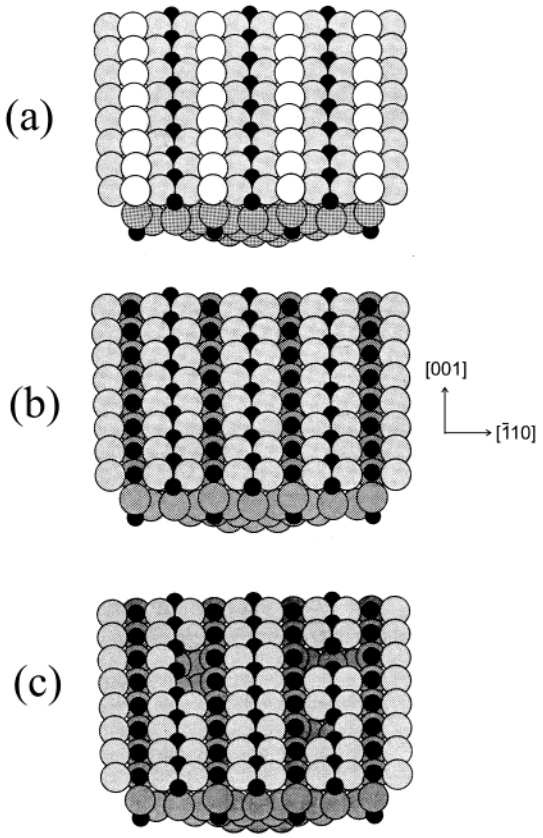

Figure 1. Ball model illustrations of SnO_2(110): (a) the ideal, stoichiometric surface, (b) the reduced surface missing all bridging oxygen anions, and (c) the defective surface with in-plane oxygen vacancies. The small solid circles represent Sn cations, whereas the large open circles represent O^{2-} anions. Increased shading of the oxygen anions represents increased depth away from the surface. The illustrations assume no relaxation.

of different compositions. The ideal, stoichiometric surface (illustrated in Figure 1a) consists of an outer atomic layer of two-coordinate oxygen anions (one coordination vacancy) that occupy bridging positions between an otherwise inaccessible, fully (six-) coordinate second layer of Sn^{4+} cations. The exposed second layer consists of five-coordinate Sn^{4+} cations (one coordination vacancy) and fully three-coordinated, in-plane oxygen anions. A nearly stoichiometric surface can be prepared by exposing an ordered surface to N_2O at 0.5 Torr and 700 K.[24] The bridging oxygens on the nearly stoichiometric surface are labile and can be removed by heating between 300 and 600 K.[14,24] A "reduced" surface can be obtained by heating the nearly stoichiometric surface to 650 K in vacuum to remove the outer atomic layer of bridging oxygen anions.[14] The removal of bridging oxygen anions exposes four-coordinate Sn^{2+} cations at the surface.[14,17,18] A ball model illustration of an ideal reduced surface is shown in Figure 1b. A "defective" surface can be prepared by argon ion bombardment and annealing to 1000 K in vacuum.[25] This treatment produces approximately 50% in-plane oxygen vacancies in what was initially the second atomic layer. The in-plane oxygen vacancies lower the coordination of the cation sites at these point defects.[25] There are enough in-plane vacancies on the defective surface to affect the local coordination shell of virtually all of the surface cations. An idealized ball model diagram of a defective surface is shown in Figure 1c. All of the illustrations in Figure 1 are based on simple terminations of the bulk structure and assume no relaxation about the vacancies.

III. Experimental Methods

The SnO_2 crystal used in this study was grown by the vapor-phase transport method of Thiel and Helbig,[26] oriented by Laue back reflection, and mechanically polished to within 1° of the (110) surface. The dimensions of the sample are approximately $4 \times 3 \times {}^1/_2$ mm^3. The SnO_2 sample was mounted on a tantalum holder that acted as an indirect heating and cooling source and provided mechanical stability. The holder was supported by two 1-mm tantalum wires connected to LN_2-cooled copper electrical feedthroughs in a sample rod manipulator. The sample temperature was monitored using a type-K thermocouple bonded directly to the back of the SnO_2 crystal with Armeco no. 569 ceramic cement. Hence, direct measurements of the crystal temperature were possible.

All experiments were performed in a turbo-pumped, dual-chamber, stainless steel ultrahigh vacuum system. The analysis chamber is equipped with a Leybold EA-11 hemispherical analyzer and a Mg anode X-ray source for X-ray photoelectron spectroscopy (XPS). The preparation chamber is equipped with a set of Vacuum Generators three-grid reverse view, low-energy electron diffraction (LEED) optics and an Inficon Quadrex 200 mass spectrometer for thermal desorption spectroscopy (TDS).

Oxidation treatments were performed using Matheson SCF grade N_2O (99.995%) at 1.3 mbar. The sample was heated to 700 K at a rate of 2 K/s, held for 2 min, and cooled to 310 K before the chamber was evacuated of N_2O. After the chamber pressure decreased to 2×10^{-9} mbar, the cryopanel was exposed to LN_2 to reduce the pressure to 4×10^{-10} mbar. To reduce the pressure into the low-to-mid-10^{-10} mbar range within a reasonable amount of time, only one oxidation treatment can be run per day.

Gas exposures were performed by backfilling the chamber through a variable leak valve. BF_3 (Aldrich, 99.5%) was used as received. For TDS experiments, a linear temperature ramp of 2 K/s was used. The low heating rate was used to minimize the possibility of thermally fracturing the ceramic SnO_2 sample. For the nearly stoichiometric surface, BF_3 was adsorbed at 190 K, whereas for the reduced and defective surfaces the exposures were performed at 170 K. Because of oxidation of the sample-holder hardware during an oxidation treatment, the nearly stoichiometric surface could not be cooled to as low an ultimate temperature as was possible following the high-temperature annealing treatments involved in the preparation of the reduced and defective surfaces. The mass spectrometer was equipped with a glass skimmer to minimize the sampling of desorption products from the crystal support hardware. During TDS experiments, the background pressure was less than 2×10^{-10} mbar between doses. Gas exposures reported in this study have *not* been corrected for ion gauge sensitivities.

XPS spectra were collected at 170 K from the nearly stoichiometric surface and at 150 K from the reduced and defective surfaces. The binding-energy scale for all reported XPS spectra has been shifted to align the Sn $3d_{5/2}$ peak to 486.4 eV.[27] All XPS experiments were run at a pass energy of 200 eV, which corresponds to an Ag $3d_{5/2}$ line width of 2.1 eV. The large pass energy was used to achieve a better signal-to-noise ratio for the boron 1s feature because boron 1s has a small X-ray absorption cross section.[28]

IV. Results

1. Thermal Desorption Spectroscopy. BF_3 adsorption was examined by TDS for the nearly stoichiometric, reduced, and defective surfaces. In simple Lewis acid/base terms, one might expect a different basicity for the nearly stoichiometric and

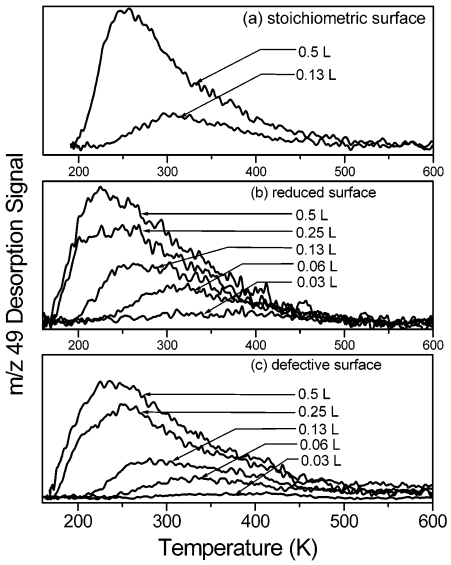

Figure 2. Thermal desorption traces for BF_3 adsorbed on (a) a nearly stoichiometric $SnO_2(110)$ surface, (b) a reduced surface, (c) and a defective surface.

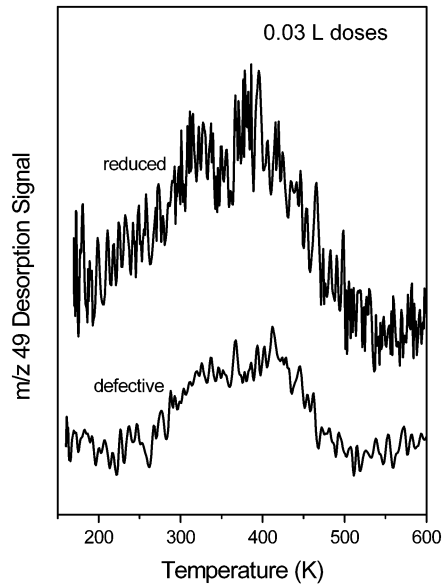

Figure 3. Thermal desorption traces for BF_3 in the low-coverage limit (0.03-L exposures) on the reduced surface and on defective $SnO_2(110)$ surfaces.

reduced surfaces because of the different types of oxygen—bridging (two-coordinate) and in-plane (three-coordinate)—exposed at these surfaces. Similarly, differences in basicity (i.e., anion electronic properties) might also be expected between the reduced and defective surfaces as a result of the introduction of in-plane oxygen vacancies adjacent to the nearest-neighbor cations of the remaining in-plane anions.

The coverage dependence of the BF_3 desorption traces from a nearly stoichiometric surface is shown in Figure 2a. At the lowest dose investigated, 0.13 L, one BF_3 desorption feature is observed with a desorption-peak temperature of about 300 K. For a 0.5-L BF_3 exposure, this feature shifts down in temperature to 250 K.

For the reduced and defective surfaces, the coverage dependences of the BF_3 desorption traces are illustrated in Figure 2b and c, respectively. In addition, traces for 0.03-L doses are shown on a more expanded scale in Figure 3 for both surfaces. For the reduced surface, BF_3 desorption occurs as a broad feature centered near 370 K for the lowest dose investigated (0.03 L). With increasing BF_3 coverage, this feature shifts down in temperature to 220 K at an exposure of 0.5 L. The coverage dependence of the BF_3 desorption traces for the defective surface is shown in Figure 2c. At the lowest dose investigated, 0.03 L, a broad BF_3 desorption feature is observed, centered around 380 K. With increasing BF_3 coverage, this feature shifts down in temperature to 250 K at an exposure of 0.5 L. The differences in desorption temperatures between surfaces are primarily dependent on the BF_3 coverage on the surface. The desorption temperature is lower with higher BF_3 coverage on all SnO_2 surfaces. (Note: TDS spectra are shown only for low (0.5 L $\geq$) BF_3 exposures because desorption signals from the sample support hardware become apparent for larger doses.)

The BF_3 desorption features from the various SnO_2 surfaces are similar. The reduced and defective surfaces that expose three-coordinate O^{2-} anions exhibit one BF_3 desorption feature that is attributed to the desorption of molecularly adsorbed BF_3 from three-coordinate O^{2-} anions. (See the XPS results and discussion below.) The desorption temperatures from the reduced and defective SnO_2 surfaces at low BF_3 coverages are similar to the desorption temperature ($\sim$370 K) reported for the formation of a Lewis acid/base adduct at three-coordinate O^{2-} anions on $Cr_2O_3(10\bar{1}2)$.[13]

A decrease in desorption temperature with coverage can be characteristic of a second-order desorption process. However, a second-order Redhead analysis[29] of the TDS data shows no linearity suggestive of second-order behavior that might indicate a recombination process for BF_3 desorption. All BF_3 desorption features are thought to originate from a molecular BF_3 adsorbate. XPS data (below) also suggests a molecular adsorbate associated with these TDS features. Assuming a normal preexponential of 10^{13} s^{-1}, the apparent first-order activation energy for desorption is estimated from the Redhead equation to be 13.5−24.5 kcal/mol for the BF_3 desorption feature seen on all SnO_2 surfaces.[29] No attempt was made to determine the preexponential independently via the method of heating rate variation. The heating rate was kept intentionally low (2 K/s) to avoid the possibility of thermal fracture of the ceramic sample.

The decrease in desorption temperature with coverage is attributed to repulsive interactions in the adlayer. Molecular BF_3 in a Lewis adduct is expected to change from a planar molecular geometry a tetrahedral geometry (similar to that of ammonia) when bound to a Lewis base.[30] Hence, adsorbed molecular BF_3 will acquire a dipole moment upon interaction with basic surface sites (i.e., surface oxygen anions). Repulsive interactions between the dipoles of BF_3 in the adlayer are the likely cause of the shift to lower temperatures of the BF_3 desorption features with increasing coverage. Similar effects are well known for NH_3 chemisorption on a variety of metal and oxide surfaces, where a similar strong dependence of desorption temperature on coverage is observed for molecular NH_3 adsorbates.[31−36]

The desorption temperatures observed for the nearly stoichiometric surface are similar to those on the reduced and defective surfaces. Unlike the case for BF_3 adsorption on $Cr_2O_3(10\bar{1}2)$ surfaces,[13] there is no evidence of significantly different desorption features at different temperatures associated with surface oxygen anions of different coordinations. The nearly-stoichiometric surface exposes two types of lattice oxygen—two-coordinate bridging oxygen and three-coordinate in-plane oxygen—but only one BF_3 desorption feature appears on this surface. No separate BF_3 desorption signal is observed that might be attributable to adsorption at two-coordinate bridging oxygens on the nearly stoichiometric surface.

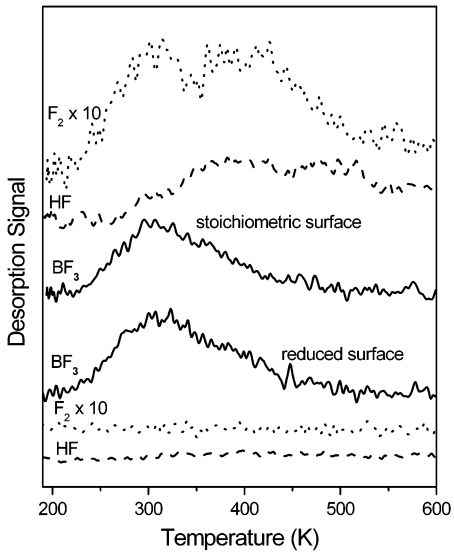

Figure 4. Thermal desorption traces for 0.13-L BF_3 exposures on the nearly stoichiometric and reduced surfaces. HF and F_2 reaction products evolve from the stoichiometric surface, but no gas-phase reaction products are seen from the reduced or defective surfaces.

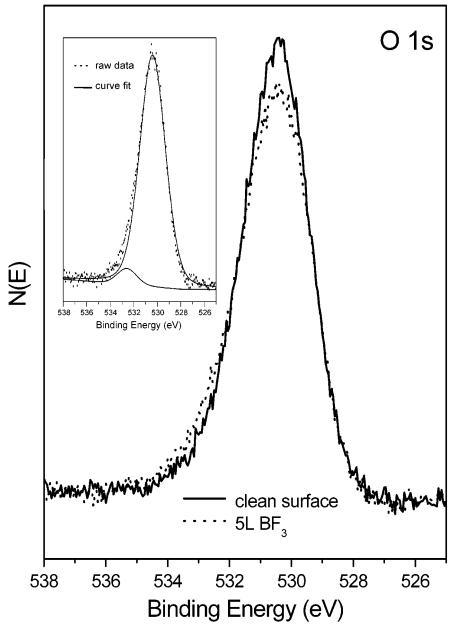

Figure 5. O 1s XPS spectra for the reduced surface before and after a 5-L exposure of BF_3. The inset shows a curve fit to the spectrum for the 5-L BF_3 exposure. A feature characteristic of lattice oxygen on the clean surface is seen in addition to a higher binding energy contribution associated with surface oxide species that form a Lewis adduct with BF_3.

Whereas the BF_3 desorption features are attributed to a molecularly adsorbed surface species, BF_3 adsorption on the different SnO_2(110) surfaces is not an entirely clean molecular adsorption/desorption process. Trace amounts of HF and F_2 are detected during each BF_3 TDS run on the nearly stoichiometric surface. Hence, some BF_3 dissociation occurs. No gas-phase reaction products are seen in TDS for the reduced and defective surfaces, even though BF_3 dissociation occurs (as shown below with XPS). A comparison of the desorption behavior seen in TDS between the nearly stoichiometric and reduced surfaces is shown in Figure 4. For a 0.13-L exposure of BF_3, the desorption traces from molecular BF_3 are nearly identical, but small amounts of HF and F_2 desorb from the nearly stoichiometric surface, whereas none is observed from the reduced surface. From the nearly-stoichiometric surface, HF desorption occurs in a broad feature in the temperature range of 350−550 K, whereas two F_2 desorption features are observed, centered at about 300 and 400 K as shown in Figure 4.

The dissociation of BF_3 results in the deposition of boron and fluorine on the surface (as shown below with XPS) after successive TDS runs. After the build up of surface boron and fluorine saturates, the "BF_3-modified" reduced and defective surfaces give a larger BF_3 desorption signal in TDS for a given exposure than observed from an initially clean surface. The boron and fluorine left on the surface decrease the probability of BF_3 dissociation in subsequent exposures, resulting in higher coverages of reversibly adsorbed molecular BF_3 for a given dose. Similar to the case of BF_3 adsorption on $Cr_2O_3(10\bar{1}2)$ surfaces,[13] the shape and desorption temperature of the TDS features from these BF_3-modified surfaces are essentially the same as those of the TDS features arising from clean surfaces when the amounts of desorbing BF_3 (i.e., the coverage of molecular BF_3) are similar. The boron and fluorine left on the reduced and defective surfaces effect the BF_3 coverage for a given exposure but not the desorption temperature for a given coverage of molecular BF_3.

2. X-ray Photoelectron Spectroscopy. O 1s. XPS was used to study the interaction of BF_3 with the nearly stoichiometric, reduced, and defective surfaces. Changes in the oxygen 1s signal upon BF_3 adsorption on SnO_2(110) surfaces were seen with XPS. These changes are shown in Figure 5 for the reduced surface only, but the spectra are representative of what is seen from all of the SnO_2 surfaces investigated. The O 1s feature on the clean surface appears at a binding energy of 530.4 ± 0.1 eV. When the surface is exposed to 5 L of BF_3, the O 1s feature decreases in intensity and broadens to higher binding energies. Curve fitting of the O 1s spectrum results in a lattice oxygen feature at 530.4 ± 0.1 eV similar to the O 1s feature on the clean surface and an additional small feature at higher binding energy. (See the inset of Figure 5.) Curve fitting gives a binding energy for this additional feature of 532.7 ± 0.1 eV for the nearly stoichiometric surface, 532.6 ± 0.1 eV for the reduced surface, and 532.2 ± 0.1 eV for the defective surface. This higher binding energy feature disappears when the sample is heated to temperatures where molecular BF_3 is removed in TDS experiments, indicating that these changes are associated with reversibly adsorbed BF_3. The higher binding energy feature indicates charge transfer from the surface oxygen to the boron atom in adsorbed BF_3 and demonstrates a direct interaction of BF_3 with surface oxygen sites to form a Lewis acid/base adduct. A similar high binding energy O 1s feature is also observed on $Cr_2O_3(10\bar{1}2)$ following molecular BF_3 adsorption at surface oxygen sites.[13]

B 1s and F 1s. The nature of the adsorbed species was also investigated by XPS. For all XPS experiments, the surfaces were exposed to 5 L of BF_3 (at 170 K for the nearly stoichiometric surface and at 150 K for the reduced and defective surfaces), heated to 300 K to remove the majority of molecular BF_3 observed in TDS, and then heated to 700 K and checked for residual boron and fluorine left from decomposed BF_3.

The B 1s spectra are shown in Figure 6, and the features are broad as a result of running at the high pass energy of 200 eV. For each of the three surfaces investigated, the binding energy of the broad B 1s feature decreases with increasing annealing temperature, suggesting that the spectra contain multiple features that are not resolved because of the low resolution of the measurements. The B 1s binding energies are listed in Table 1.

For the reduced and defective surfaces, the binding energies

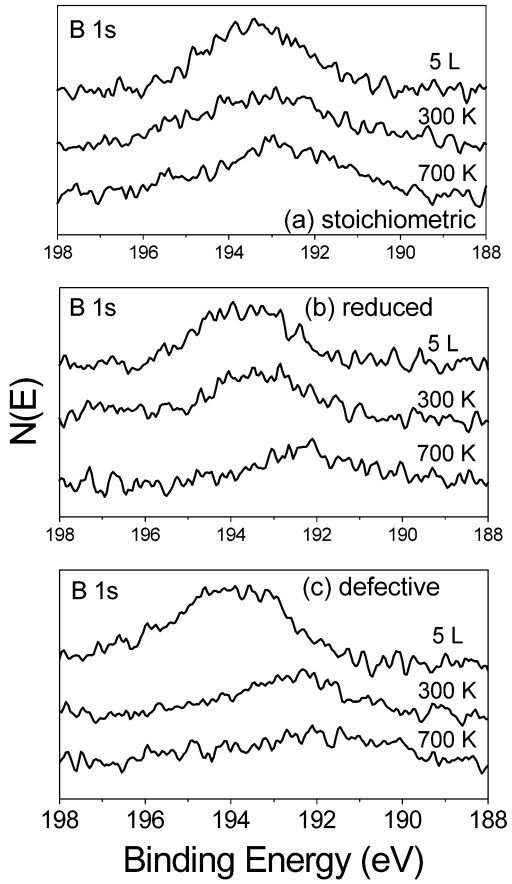

Figure 6. B 1s XPS spectra taken following a 5-L BF_3 exposure with subsequent heating to 300 K (to remove the molecular BF_3 seen in TDS) and 700 K for (a) a nearly stoichiometric $SnO_2(110)$ surface, (b) a reduced surface, and (c) a defective surface.

TABLE 1: B 1s Binding Energies on $SnO_2(110)$ Surfaces

sample preparation	5-L BF_3	300 K	700 K
nearly stoichiometric surface	193.4 eV	193.2 eV	192.8 eV
reduced surface	193.7 eV	193.3 eV	192.2 eV
defective surface	194.0 eV	192.7 eV	192.0 eV

for residual boron left on the surface after heating to 700 K are similar: 192.2 and 192.0 eV, respectively. These B 1s binding energies fall in the range of 192.0−192.3 eV reported for boron adatoms on $Cr_2O_3(10\bar{1}2)$[13] and suggest the desorption of reversibly (molecularly) adsorbed BF_3 and the complete dissociation of irreversibly adsorbed BF_3 at this temperature. Interestingly, heating to a similar temperature following adsorption on the nearly stoichiometric surface results in a significantly higher B 1s binding energy of 192.8 eV, suggesting something in addition to boron adatoms following complete BF_3 decomposition on the stoichiometric surface. We attribute the higher binding energy for residual boron on the stoichiometric surface (after annealing to 700 K) to the formation of a surface boron oxide since the binding energy (192.8 eV) falls in the range of 192.0−193.3 eV reported for boron oxide.[27,37,38]

The higher binding energies observed for all surfaces following a 5-L dose and the decrease to intermediate binding energies after heating to remove most of the molecular species observed in TDS suggest unresolved higher binding energy contributions to the spectra including molecular BF_3 and BF_X fragments. Note that B 1s binding energies of 194.9 and 194.3 eV have been observed for BF_3 in the acid/base adducts NH_3/BF_3 and C_5H_5N/BF_3, respectively,[27] and that ∼194 eV has been observed for molecular BF_3 adsorbed at surface oxygen anions

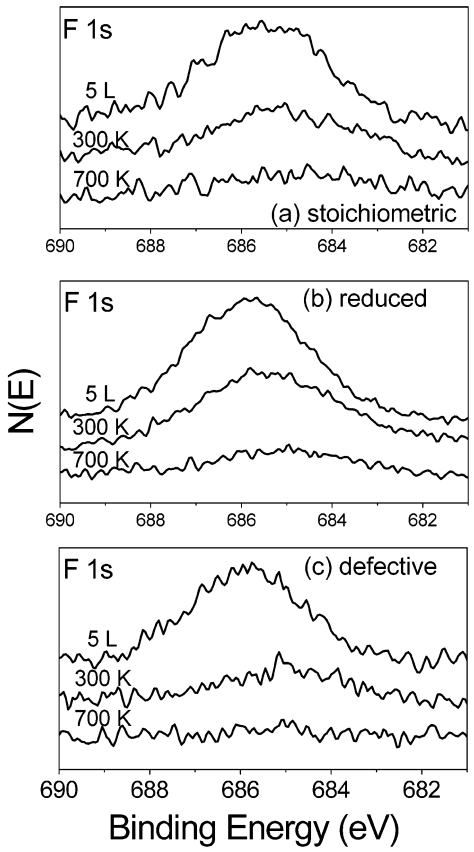

Figure 7. F 1s XPS spectra taken following a 5-L BF_3 exposure with subsequent heating to 300 K (to remove the molecular BF_3 seen in TDS) and 700 K for (a) a nearly stoichiometric $SnO_2(110)$ surface, (b) a reduced surface, and (c) a defective surface.

TABLE 2: F 1s Binding Energies on $SnO_2(110)$ Surfaces

sample preparation	5-L BF_3	300 K	700 K
nearly stoichiometric surface	685.5 eV	685.1 eV	684.9 eV
reduced surface	685.9 eV	685.5 eV	685.0 eV
defective surface	685.9 eV	685.0 eV	685.0 eV

on $Cr_2O_3(10\bar{1}2)$.[13] The observed binding energies following an initial 5-L dose suggest that a molecular adsorbate can account for the unresolved high binding energy component of the B 1s feature that is removed by heating to temperatures where BF_3 desorption is observed in the TDS experiments.

The fluorine 1s XPS region is shown in Figure 7 for the nearly stoichiometric surface, the reduced surface, and the defective surface along with binding energies for the F 1s features in Table 2. Following an exposure of 5 L of BF_3, one F 1s feature appears at a binding energy of 685.5 eV for the nearly stoichiometric surface, at 685.9 eV for the reduced surface, and at 685.9 eV for the defective surface. Fluorine in the acid/base adduct NH_3/BF_3 has a reported F 1s binding energy of 686.6 eV.[27] The broad F 1s features shown in Figure 7 following a 5-L BF_3 dose clearly contain a high binding energy component that overlaps with this range, suggestive of a molecular surface species. After annealing the exposed surface to 700 K, the F 1s features shifts to lower binding energies of 684.9 eV for the nearly-stoichiometric surface, 685.0 eV for the reduced surface, and 685.0 eV for the defective surface. The shift to lower binding energies to give similar values for the F 1s feature on all surfaces after removing molecular BF_3 indicates residual surface fluorine from dissociated BF_3. The range of 684.9−685.0 eV for the F 1s feature after annealing to 700 K falls in the range of values for a variety of metal fluoride compounds (i.e., MnF_2 and CuF_2),[27]

indicating that fluorine from dissociated BF_3 is likely bound at surface metal (i.e., Sn) sites. These details are comparable to the F 1s XPS results seen from BF_3 adsorption on $Cr_2O_3(10\bar{1}2)$ surfaces.[13]

V. Discussion

The reduced and defective surfaces expose predominantly one type of surface oxygen, three-coordinate O^{2-} anions. In TDS, the desorption features at 370−380 K for a low BF_3 coverage are attributed to the desorption of BF_3 from these three-coordinate O^{2-} anions. The similarity in desorption temperatures observed on the reduced and defective surfaces indicates that the introduction of in-plane oxygen vacancies has little effect on the interaction of BF_3 with the remaining in-plane anions. This observation suggests that the electronic properties of three-coordinate in-plane anions are not significantly impacted by the presence of oxygen vacancies adjacent to their nearest-neighbor tin cations (i.e., nearest neighbor cations of lower coordination).

In addition, the BF_3 desorption features observed on the reduced and defective surfaces are similar to the BF_3 desorption features seen at 370 K on stoichiometric $Cr_2O_3(10\bar{1}2)$. These features have also been attributed to desorption from three-coordinate O^{2-} anions.[13] Hence, it appears that a similar coordination environment for the surface oxygen anions on $SnO_2(110)$ and $Cr_2O_3(10\bar{1}2)$ gives rise to a similar desorption temperature in TDS in the low coverage limit. Experiments on other oxide surfaces will be required before it can be determined if this agreement is simply fortuitous or indicative of a more general electronic similarity in three-coordinate surface oxygen anions of other materials.

The nearly stoichiometric surface exposes two types of anions: two-coordinate bridging and three-coordinate in-plane O^{2-} anions. In Figure 2, no apparent differences in BF_3 desorption behavior are seen between the nearly stoichiometric surface and the reduced and defective surfaces that expose only three-coordinate in-plane O^{2-} anions. However, differences are seen for the nearly stoichiometric surface in the B 1s XPS data and TDS reaction products. The observation of boron oxides in XPS and F_2 and HF gas-phase products in TDS, none of which are observed for the reduced and defective surfaces, suggests that the reaction products generated by the stoichiometric surface result from the irreversible reaction of BF_3 with the labile two-coordinate bridging oxygen on the stoichiometric surface. The hydrogen in the HF product probably originates from a small amount of adsorbed water from the background resulting from the high-pressure oxidation and prolonged pump down time required to produce a stoichiometric surface.

The lack of any additional BF_3 desorption features in TDS (Figure 2) that may be attributed to adsorption at two-coordinate bridging oxygens on the nearly stoichiometric surface can be explained by the lower thermal stability of these bridging oxygen species. Whereas TDS readily distinguishes between BF_3 desorption from thermally stable three-coordinate and terminal oxygen (Cr═O) on the $Cr_2O_3(10\bar{1}2)$ surface,[13] it does not give any direct indication of the two-coordinate bridging oxygen anions on stoichiometric $SnO_2(110)$ in the BF_3 desoprtion trace. The primary difference between the situation with SnO_2 and the previously investigated case of Cr_2O_3 is that the bridging oxygen on the stoichiometric surface is labile and can be removed by heating between 300 and 600 K.[24] Hence, it is likely that the lower thermal stability of the two-coordinate bridging oxygen anions is related to the apparent reactivity of these species with BF_3 and their tendency to react irreversibly rather than form a reversible Lewis acid/base adduct upon adsorption as seen with three-coordinate anions. Given that an irreversible reaction occurs between BF_3 and the labile bridging oxygen, it is understandable that a simple molecular adsorption/desorption signature is not observed in TDS for the interaction of BF_3 with bridging oxygen on stoichiometric $SnO_2(110)$.

Conclusions

BF_3 has been used to probe the basicity of surface oxygen anions on $SnO_2(110)$ surfaces. BF_3 interacts molecularly with three-coordinate surface oxygen on $SnO_2(110)$ to form a Lewis acid/base adduct, and thermal desorption provides a reasonable measure of the basicity of these thermally stable three-coordinate O^{2-} anions. The desorption temperature in the zero-coverage limit from three-coordinate anions is remarkably similar to that observed from three-coordinate oxygen anions on $Cr_2O_3(10\bar{1}2)$. However, BF_3 reacts irreversibly with the more labile two-coordinate bridging oxygen, and no distinctive BF_3 desorption feature is observed in TDS that can be used to provide a measure of the basicity of bridging oxygen anions on $SnO_2(110)$. Instead, the gas-phase reaction products HF and F_2 are observed in TDS, along with boron oxide formation. These results indicate that the applicability of BF_3 thermal desorption as a probe of O anion basicity may be limited in cases where the thermal stability of the anions is low. As on $Cr_2O_3(10\bar{1}2)$,[13] the use of BF_3 as a probe molecule is complicated by some dissociation and the slow build up of surface boron and fluoride during consecutive thermal desorption runs.

Acknowledgment. We gratefully acknowledge financial support by the Chemical Sciences, Geosciences and Biosciences Division, Office of Basic Energy Sciences, Office of Science, U.S. Department of Energy through grant DE-FG02-97ER14751. We also thank Professor J.-M. Gilles (Facultés Universitaires Notre-Dame de la Paix, Namur) for providing the single crystal used in this study.

References and Notes

(1) Barteau, M. A. *J. Vac. Sci. Technol., A* **1993**, *11*, 2162.
(2) Stair, P. C. *J. Am. Chem. Soc.* **1982**, *104*, 4044.
(3) Tanabe, K. *Solid Acids and Bases*; Academic Press: New York, 1970.
(4) Tanabe, K.; Misono, M.; Hattori, H. *New Solid Acids and Bases: Their Catalytic Properties*; Elsevier: Amsterdam, 1989.
(5) Knozinger, H. *Adv. Catal.* **1976**, *25*, 184.
(6) Cardona-Martinez, N.; Dumesic, J. A. *Adv. Catal.* **1992**, *38*, 149.
(7) Auroux A.; Gervasini, A. *J. Phys. Chem.* **1990**, *94*, 6371.
(8) Zhang, G.; Hattori, H.; Tanabe, K. *Appl. Catal.* **1988**, *36*, 189.
(9) Abee, M. W.; York, S. C.; Cox, D. F. *J. Phys. Chem. B* **2001**, *105*, 7755.
(10) Freund, H.-J.; Roberts, M. W. *Surf. Sci. Rep.* **1996**, *25*, 225.
(11) Seiferth, O.; Wolter, K.; Dillmann, B.; Klivenyi, G.; Freund, H.-J.; Scarano, D.; Zecchina, A. *Surf. Sci.* **1999**, *421*, 176.
(12) Au, C. T.; Hirsch, W.; Hirschwald, W. *Surf. Sci.* **1988**, *199*, 507.
(13) Abee, M. W.; Cox, D. F. *J. Phys. Chem. B* **2001**, *105*, 8375.
(14) Cox, D. F.; Fryberger, T. B.; Semancik, S. *Phys. Rev. B* **1988**, *38*, 2072.
(15) Cox, D. F.; Fryberger, T. B.; Semancik, S. *Surf. Sci.* **1989**, *224*, 121.
(16) Cox, D. F.; Fryberger, T. B. *Surf. Sci.* **1990**, *227*, L105.
(17) Cox, P. A.; Egdell, R. G.; Harding, C.; Patterson, W. R.; Tavener, P. J. *Surf. Sci.* **1982**, *123*, 179.
(18) Themlin, J. M.; Sporken, R.; Darville, J.; Caudano, R.; Gilles, J. M.; Johnson, R. L. *Phys. Rev. B* **1990**, *42*, 11914.
(19) Jones, F. H.; Dixon, R.; Foord, J. S.; Egdell, R. G.; Pethica, J. B. *Surf. Sci.* **1997**, *376*, 367.
(20) Pang, C. L.; Haycock, S. A.; Raza, H.; Møller, P. J.; Thornton, G. *Phys. Rev. B* **2000**, *62*, R7775.
(21) Atrei, A.; Zanazzi, E.; Bardi, U.; Rovida, G. *Surf. Sci.* **2001**, *475*, L223.

(22) Sinner-Hettenbach, M.; Göthelid, M.; Weissenrieder, J.; von Schenck, H.; Weiss, T.; Barsan, N.; Weimar, U. *Surf. Sci.* **2001**, *477*, 50.
(23) Sinner-Hettenbach, M.; Göthelid, M.; Weiss, T.; Barsan, N.; Weimar, U.; von Schenck, H.; Giovanelli, L.; Le Lay, G. *Surf. Sci.* **2002**, *499*, 85.
(24) Gercher, V. A.; Cox, D. F.; Themlin, J.-M. *Surf. Sci.* **1994**, *306*, 279.
(25) Gercher, V. A.; Cox, D. F. *Surf. Sci.* **1994**, *312*, 106.
(26) B. Thiel, B.; Helbig, R. *J. Cryst. Growth* **1976**, *32*, 259.
(27) Moulder, J. F.; Stickle, W. F.; Sobol, P. E.; Bomben, K. D.; Chastain, J. *Handbook of X-ray Photoelectron Spectroscopy*; Perkin-Elmer: Eden Prairie, MN, 1992.
(28) The Leybold sensitivity factor for B 1s is 0.101.
(29) Redhead, P. A. *Vacuum* **1962**, *12*, 203.
(30) Booth, H. S. *Boron Trifluoride and Its Derivatives*; Wiley & Sons: New York, 1949.
(31) Sexton, B. A.; Mitchell, G. E. *Surf. Sci.* **1980**, *99*, 523.
(32) Benndorf, C.; Madey, T. E. *Surf. Sci.* **1983**, *135*, 164.
(33) Wu, M.-C.; Truong, C. M.; Goodman, D. W. *J. Phys. Chem.* **1993**, *97*, 4182.
(34) Van Hardeveld, R. M.; van Santen, R. A.; Niemantsverdriet, J. W. *Surf. Sci.* **1996**, *369*, 23.
(35) Chrysostomou, D.; Flowers, J.; Zaera, F. *Surf. Sci.* **1999**, *439*, 34.
(36) Abee, M. W.; Cox, D. F. *Surf. Sci.* **2002**, *520*, 65.
(37) Brainard, W. A.; Wheeler, D. R. *J. Vac. Sci. Technol.* **1978**, *15*, 1801.
(38) Nefedov, V. I.; Gati, D.; Dzhurinskii, B. F.; Sergushin, N. P.; Salyn, Y. V. *Zh. Neorg. Khim.* **1975**, *20*, 2307.